

Ocean physics and nutrient fields along 180° during an El Niño–Southern Oscillation cold phase

Gérard Eldin

Laboratoire d'Etudes en Géophysique et Océanographie Spatiales (CNES, CNRS, IRD, UPS), Toulouse, France

Martine Rodier

Institut de Recherche pour le Développement, Nouméa, New Caledonia

Received 30 November 2000; revised 25 September 2001; accepted 13 March 2003; published 31 October 2003.

[1] This paper presents physical and nutrient results from the Etude du Broutage en Zone Equatoriale cruise, conducted in the equatorial Pacific along the 180° meridian from 8°S to 8°N. Cold conditions of the El Niño–Southern Oscillation cycle were evident during the cruise (October–November 1996), and the equatorial upwelling was in its far western extension. Along the sampled section the nutrient-enriched area was asymmetric around the equator, and a zone of high remineralization was found from 6° to 3°S. Intensive sampling at two 5-day time series stations (3°S and 0°) provided some insight on high-frequency variability. At 3°S a deep density mixed layer showed only small fluctuations in nutrients. On the equator a rapid reduction of surface nutrients during the time series station was attributed to advection of a different water mass from the northeast, in the southward branch of a Tropical Instability Wave (TIW). Measurements from the Tropical Atmosphere–Ocean (TAO) array in the area confirmed significant contemporaneous TIW activity, which was linked to the cold conditions. Thus, in contrast to previous observations, it is shown that TIWs can contribute to relative decrease of nutrients at the equator. During the two time series sampling efforts, variability at diurnal and semidiurnal periods were found in physical parameters, originating from surface atmospheric forcing and internal wave activity at tidal frequency, respectively. In the 0–150 m layer, where intensive sampling of nutrients was performed, high-frequency variability did not seem to modify nutrient distribution significantly and physical influences dominated over biology. *INDEX TERMS:* 4231 Oceanography: General: Equatorial oceanography; 4572 Oceanography: Physical: Upper ocean processes; 4845 Oceanography: Biological and Chemical: Nutrients and nutrient cycling; *KEYWORDS:* nutrients, tropical instability waves

Citation: Eldin, G., and M. Rodier, Ocean physics and nutrient fields along 180° during an El Niño–Southern Oscillation cold phase, *J. Geophys. Res.*, 108(C12), 8137, doi:10.1029/2000JC000746, 2003.

1. Introduction

[2] Like the tropical regions of other oceans, the equatorial Pacific is characterized by a persistent upwelling tongue issuing from the horizontal Ekman divergence of surface waters under the continual westward forcing of tropical trade winds. The strength of the upwelling and the two-dimensional extension of the upwelling tongue are subject to high variability at different timescales. This variability, in turn, impacts the biology of the equatorial ocean by modifying the supply and distribution of nutrients in the euphotic layer as well as physical parameters.

[3] At scales of a few years, variability in the equatorial Pacific is dominated by El Niño–Southern Oscillation (ENSO) events. During the warm phase of ENSO, warm surface waters from the western Pacific “Warm Pool” extend toward the central Pacific, where equatorial upwell-

ing is abated or suppressed. During the cold phase (“La Niña”), the Warm Pool retreats and the equatorial upwelling tongue intensifies and extends westward. The boundary between the Warm Pool and the upwelling tongue (often defined by the 29°C SST isotherm) moves between 165°E and 150°W at different phases of the ENSO cycle [Picaut *et al.*, 1996]. Within that area, alternating water masses and dynamic regimes lead to different biological responses.

[4] The hydrology and nutrients of Warm Pool waters have been extensively described [Radenac and Rodier, 1996; Mackey *et al.*, 1997; Turk *et al.*, 2001], and numerous studies have investigated the physical and biological properties of the Pacific cold tongue during moderately warm or cold conditions [i.e., McPhaden and Hayes, 1990; Murray *et al.*, 1995]. In addition, the influence of strong ENSO warm phases on the equatorial upwelling tongue are well described for the 1982–1983 and 1997–1998 events [Barber and Kogelschatz, 1989; Chavez *et al.*, 1999]. In contrast, because conditions of strong cold phases appear to have been less frequent since the mid-1970s [Trenberth and

Hurrell, 1994], recent studies of these conditions and the maximal westward extension of the Warm Pool are limited. Including early work at 165° – 170° E [Magnier *et al.*, 1973], Radenac and Rodier [1996] studied the effects of the 1988–1989 La Niña episode at 165° E, Le Borgne *et al.* [1999] and Turk *et al.* [2001] described the 1996 cold phase conditions in the western and central Pacific, and Chavez *et al.* [1999] explored chemical and biological consequences of the 1998 La Niña in the eastern Pacific.

[5] Besides the ENSO cycle, variability at shorter periods can affect properties of the cold tongue. A strong seasonal cycle in surface physics exists in the east [McPhaden and Taft, 1988], but its influence is less noticeable west of 160° W. Intraseasonal equatorial Kelvin waves propagate across the Pacific with 40–60 day periods, affecting the depth of the thermocline and nitracline between 4° S and 4° N [Kessler *et al.*, 1995]. At shorter timescales (15–35 days) tropical instability waves (TIWs) are important for the three-dimensional advection of physical and chemical properties in surface layers [Flament *et al.*, 1996; Foley *et al.*, 1997]. Detailed dynamics of these waves is still a subject of debate [Masina and Philander, 1999], but numerous papers describe TIW observations [see Qiao and Weisberg, 1995]. To our knowledge, TIWs have not been reported westward of 155° W. At higher frequencies, gravity waves (4–5 days) have been described in the central Pacific [Eriksen, 1982], but their possible action on nutrients and biology is undocumented. Last, atmospheric forcing of a diurnal cycle in the surface modifies vertical mixing properties [Peters *et al.*, 1994], and internal waves at tidal frequency can cause important oscillations in the thermocline [Gourdeau, 1998].

[6] The Etude du Broutage en Zone Equatoriale (EBENE) cruise was carried out in October–November 1996 along the 180° meridian, at the end of the 1995–1996 cold phase of ENSO [Le Borgne and Landry, 2003]. It therefore provided an opportunity to sample the cold tongue in its far westward extension. In this paper, we show that the physics and nutrient fields at 180° were affected by several of the above mentioned mechanisms of variability, from ENSO to the semidiurnal. We further investigate the relationships between these fields at the different timescales involved, with emphasis on the TIW influence and short-term variability during 5 days of sampling at the equator. The following section describes the approach to data collection and analysis. Section 3 presents the results of sampling observations along the equatorial section from 8° S to 8° N and two time series stations at 3° S and the equator. Last, section 4 discusses the present findings in relation to climatology and previous observations.

2. Data and Analytical Methods

[7] The EBENE cruise of R/V *L'Atalante* departed from Nouméa, New Caledonia on 21 October 1996, and the equatorial section at 180° and time series stations were occupied from 25 October to 12 November 1996. Along the section, stations were occupied every degree of latitude from 8° S to 8° N, with shallow CTD casts (0–300 m) and water sampling at 12 depths. At the time series stations, an intensive sampling scheme was designed for simultaneous study of the diurnal cycles of physical, nutrient and planktonic parameters. Casts with a Sea-Bird SBE-911plus CTD

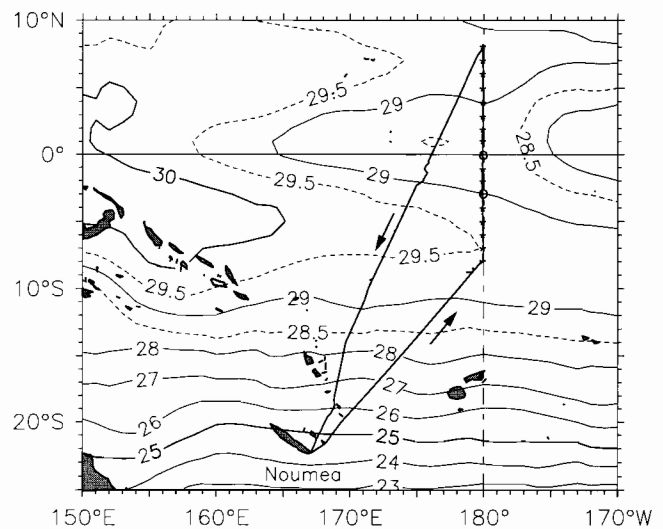


Figure 1. EBENE cruise track in the western Pacific, 21 October to 21 November 1996, overlaid on the November 1996 mean surface temperature from National Center for Environmental Prediction (NCEP).

system and 24-bottle Sea-Bird Carousel™ were taken hourly for the first 48 hours. For the remaining three days, the cast frequency was every 3 hours. Figure 1 presents a sketch of the cruise track overlaid on the monthly mean sea surface temperature map for November 1996 obtained from the National Center for Environmental Prediction (NCEP) [Reynolds and Smith, 1994].

[8] CTD profiles of temperature, salinity and oxygen were processed to 2 dbar vertical resolution and validated after laboratory calibration of sensors. Seawater bottle samples were analyzed immediately for nitrate (NO_3), nitrite (NO_2), ammonia (NH_4), phosphate (PO_4) and silicic acid ($\text{Si}(\text{OH})_4$) with a Technicon Autoanalyzer™ using colorimetric methods and routine analytical procedures as detailed by Bonnet [1995]. The lower limits of detection of the various analyses are: $0.003 \mu\text{M}$ for NO_2 , $0.003 \mu\text{M}$ for NO_3 ($<1.5 \mu\text{M}$) and $0.02 \mu\text{M}$ for NO_3 ($>1.5 \mu\text{M}$), $0.02 \mu\text{M}$ for NH_4 , $0.01 \mu\text{M}$ for PO_4 , $0.05 \mu\text{M}$ for $\text{Si}(\text{OH})_4$. All nutrients were analyzed at each station along the transect. During the time series stations only NO_3 , NO_2 and NH_4 were obtained at the full temporal resolution, while $\text{Si}(\text{OH})_4$ and PO_4 were analyzed about twice a day and only during the second half of the 5-day stations.

[9] Continuous records of upper ocean currents were obtained from the simultaneous use of two RD Instruments ADCPs, a long range 75 kHz model with a vertical resolution of 16 m and a short-range 300 kHz instrument of 4-m resolution. Velocity profiles were averaged in 5-m ensembles for both instruments. The two data sets were processed separately using the CODAS software [Bahr *et al.*, 1989]. Previous work has shown that data from these 2 instruments can be merged to provide increased vertical resolution in the upper layers [Eldin *et al.*, 1997]. However, processing for this cruise revealed a malfunctioning beam in the 300 kHz profiler, limiting high-resolution data to the 14 to 80 m depth layer. More details on data processing and other measurements obtained during the EBENE cruise can be found in the cruise report [Le Borgne *et al.*, 1998].

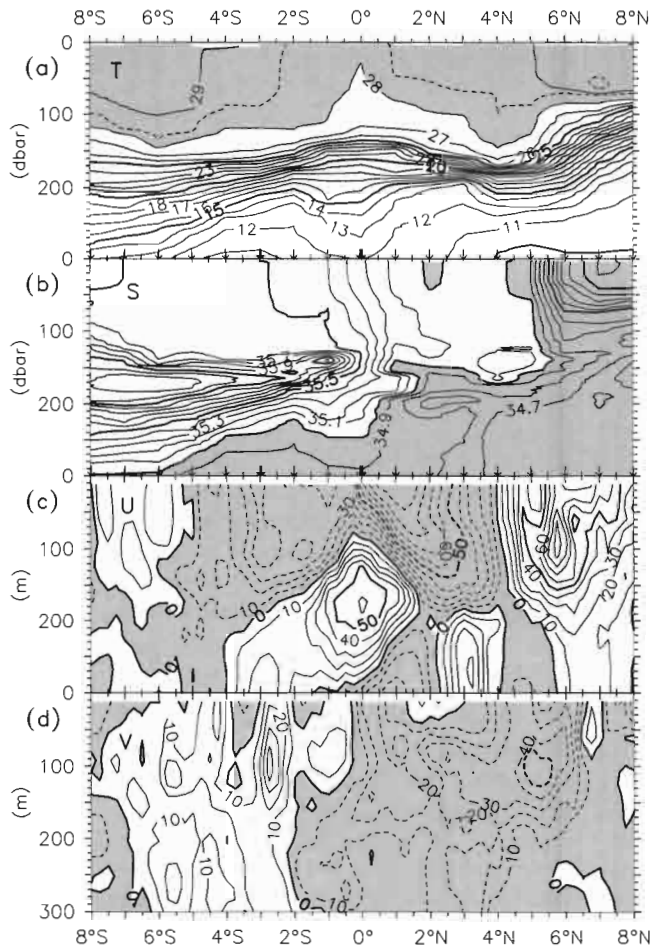


Figure 2. Meridional sections from 8°S to 8°N at 180° during the EBENE cruise: (a) temperature, (b) salinity and (c) zonal and (d) meridional velocity. CTD casts positions are shown by arrows. Isotherms are drawn every 1°C, with additional dashed lines for the 28.5° and 29.5°C isotherms. Isohalines are drawn every 0.1 psu. Current speeds are drawn at intervals of 10 cm s⁻¹. Eastward and northward flows are positive; westward and southward flows are negative.

Oceanographic and meteorological observations from the Tropical Atmosphere-Ocean (TAO) array of buoys also help in the interpretation of the present results. These data are made freely available by the TAO Project Office, NOAA, Seattle, Washington, USA.

3. Results

3.1. Cross-Equatorial Section at 180°

[10] Figures 2a–2d present sections of hydrology and currents along the 180° transect. Above the thermocline, the temperature distribution was quasi-symmetrical around the equator, with two warm regions (>29°C) south of 4°S and north of 5°N, and relatively colder waters in between. At the base of the homogeneous surface layer and poleward of 2° latitude, the 28°C isotherm defined the top of the thermocline. It was uplifted and almost reached the surface at the equator, where a local temperature minimum of 28.1°C was observed. This equatorial “chimney” is a

typical feature of wind-driven equatorial upwelling [i.e., *Wyrtki and Kilonsky, 1984*]. The homogeneous warm temperature layer was generally deeper to the south, except for an isolated deepening to 150 m at 4°N. Under these warm waters, the upper thermocline (centered on the 20°C isotherm) rose from about 200 m at 8°S to 120 m at 8°N. Well known features of the central Pacific tropical thermocline were also observed, including a slow northward slope south of 2°S, a spreading of the 12°–27°C isotherms around the equator, a deepening and sharpening at 3°–4°N and a steeper meridional slope north of 4°N. These features are signatures of the geostrophic zonal circulation: the South Equatorial Current (SEC) and the North Equatorial Countercurrent (NECC) at the surface, and the eastward Equatorial Undercurrent (EUC), South Subsurface Countercurrent (SSCC), and North Subsurface Countercurrent (NSCC) in and below the thermocline.

[11] South of the equator and above the 28°C isotherm, salinity (Figure 2b) was also homogeneous, varying from 35.4 to 35.7. North of the equator, a meridional gradient appeared and intensified northward, with a characteristic NECC minimum of less than 34.5 north of 5.5°N. In the thermocline, the high-salinity tongue of Tropical Water [*Tsuchiya, 1968*] ended with a meridional gradient between 1°S and 1°N.

[12] The section of measured zonal currents (Figures 2c and 2d) confirmed features of the geostrophic zonal circulation already evident from the temperature and salinity distributions. In contrast, measured meridional components gave details of the circulation that could not be computed from geostrophy. South of 5°S, for instance, the South Equatorial Counter Current (SECC) of 0–10 cm s⁻¹ was associated with the deepening of the warmest surface waters and a very weak and variable meridional component. From 5°S to 4°N, the westward SEC was found above the thermocline, straddling the eastward EUC with its two ‘legs’ at 3°S and 3°N (SSCC, NSCC). Between 0° and 2°N and under the EUC, the upper part of the Equatorial Intermediate Current (EIC) reached 30 cm s⁻¹ [*Delcroix and Hénin, 1988*]. The SEC had a maximum velocity of more than 90 cm s⁻¹ in surface north of the equator while it stayed under 50 cm s⁻¹ in the south. In addition, its meridional component (northward in the south, southward in the north) showed a convergence on the equator, opposing the transport associated with active upwelling. These points will be discussed in section 4 and related to high-frequency variability observed during the equatorial time series station. The EUC core was centered at the equator, 170 m deep, with a zonal velocity of 60 cm s⁻¹ and a slight southward component. North of 4°N, the NECC extended from the surface to deeper than 300 m, with a strong southeastward maximum of more than 100 cm s⁻¹ at 80–100 m and a complicated fine structure.

[13] The signature of the upwelling zone defined from the temperature distribution was also evident in enhanced surface nutrients (Figures 3a–3e); the physical and chemical structures of these upwelled waters superimposed on the low concentrations of phytoplankton biomass (0.1 to 0.35 mg m⁻³), [*Le Bouteiller et al., 2003*] are characteristic of a high-nutrient, low-chlorophyll (HNLC) area [*Minas et al., 1986*]. The NO₃-enriched surface waters defined by the 0.1 μM isoline extended over 13 degrees of latitude from

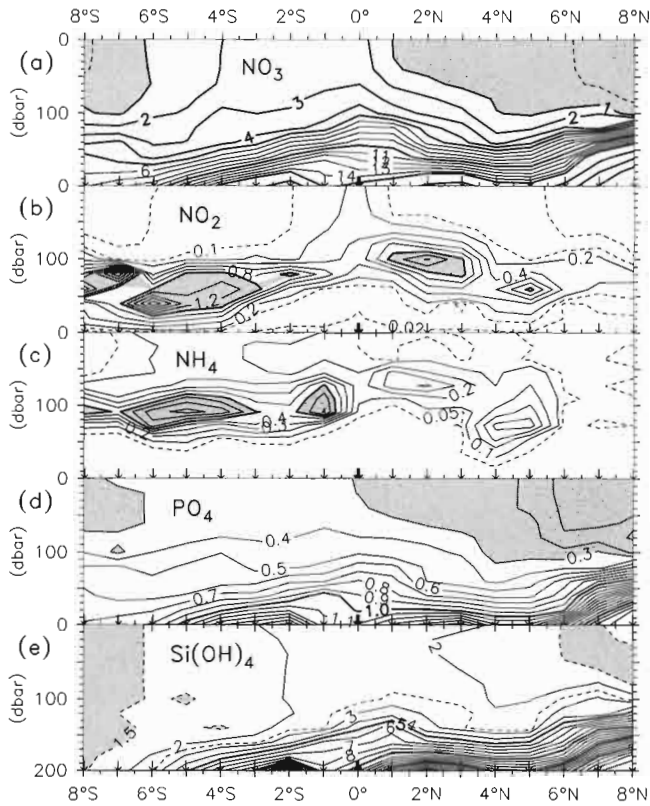


Figure 3. As in Figure 2 except for (a) nitrate, (b) nitrite, (c) ammonia, (d) phosphate, and (e) silicic acid. Nutrient units are μM .

7°S to 6°N and was somewhat asymmetrically distributed, with higher values toward the south. This asymmetry is a classical structure in the western [Radenac and Rodier, 1996] and central Pacific [Murray et al., 1995; Raimbault et al., 1999]. However, it was reinforced here by an unusually low meridional gradient of nitrate over 5 degrees of latitude north of the equator ($0.2 \mu\text{M deg}^{-1}$). In the subsurface, the meridional distribution of NO_3 at 180° was also quite standard and similar to those described along 165°E [Radenac and Rodier, 1996]. Thus the spreading of isolines was evident between 160 and 200 m in the 2°S – 2°N equatorial band, which is consistent with the geostrophic signature of the EUC. At depth, the lowest NO_3 concentrations and the weakest vertical NO_3 gradient were observed in the southern part of the transect ($\text{NO}_3 < 8 \mu\text{M}$ at 200 m), while highest values were found in the north ($\text{NO}_3 > 20 \mu\text{M}$ at 200 m).

[14] Subsurface maxima of NO_2 and NH_4 were present on each side of the upwelling but were much more developed in the south than in the north. The highest concentrations for both nutrients reached more than $1 \mu\text{M}$. As a general rule, the NO_2 distribution showed a sharp maximum at the top of the nitracline, while the NH_4 profiles were relatively smooth with a flat maximum above the NO_2 peak. Between 6°S and 1°S , NH_4 was present up to the surface with a high subsurface maximum, which is the sign of intense remineralization. High heterotrophic biomasses at these latitudes, i.e., bacteria [Brown et al., 2003] and zooplankton [Le Borgne et al., 2003], and a relative minimum in oxygen

concentration (not shown), are consistent with local regeneration of organic matter. Meridional asymmetry of remineralization products is addressed in section 4.

[15] Phosphate followed the same general distribution pattern as nitrate, with a north-south asymmetry, low subsurface values and gradients in the south, and high subsurface values and gradients in the north. However, in contrast to nitrate, phosphate was never depleted in surface and was still present outside of the nitrate-enriched area, especially in the southernmost part of the transect ($>0.25 \mu\text{M}$). This distribution is similar to other observations in the central Pacific [Murray et al., 1995; Raimbault et al., 1999]. Silicic acid distribution has been extensively described by Leynaert et al. [2001] and will not be detailed here. We note, however, that the distribution of $\text{Si}(\text{OH})_4$ in the temperature homogeneous layer was roughly centered at the equator, in contrast to other nutrients. In addition, the Si/N molar ratio, defined as an index of decoupling between nitrogen and silicium recycling, was <1 at the base of the temperature homogeneous layer all along the section and up to the surface between 5°S and 1°S [Leynaert et al., 2001, Figure 2c]. These define the areas of disproportionately high nitrogen remineralization.

3.2. Time Series Station at 3°S , 180°

[16] A 5-day time series station was occupied at 3°S , 180° from 28 October, 2100 LT, to 2 November, 1600 LT. For easier comprehension of diurnal cycles, we maintain a local time reference (TU + 12) in discussing these results.

[17] The temperature time series (Figure 4a) showed a weak diurnal cycle of amplitude 0.2°C in the upper 20 m during the first 2 days, its amplitude increasing subsequently to 0.4°C . A deepening of the surface homogeneous layer by about 30 m was observed during the last 2 d of sampling. At the same time, some stratification was evident as a 0.1°C warming of the first 50 m, under the surface diurnal stratification, even during local nighttime. This was also observed for salinity, where a freshening of about 0.1 appeared at the same time at the top of an otherwise very homogeneous salinity field in the surface layer. At depth, the thermocline and halocline did not significantly deviate from 150 m during the station. The current time series (Figures 4c and 4d) showed the SEC above 200 m and the EUC below, with high-frequency variability of about 10 cm s^{-1} . In the meridional velocity section, a more coherent pattern of variability at scales of about 12 hours strengthened after 29 October, with maximum amplitude of 8 cm s^{-1} at the base of the SEC between 120 and 150 m. This variability was most probably linked to internal waves at the tidal frequency, which are often triggered by interactions of the tidal barotropic signal with topography [Gourdeau, 1998]; in our case, neighboring island chains are likely involved. On average, the currents were slightly southward in the first 50 m, and northward at 100–200 m depth, above the EUC. The latter was coherent with active equatorial upwelling 3 degrees north of that station.

[18] At this station, NO_3 (and PO_4 , not shown) distribution (Figure 5a) did not display any clear overall trend during 5 days, except a slow deepening of the nitracline from 100 to 150 m during the two last days in association with the hydrology. The lack of large changes during this time series station was also evident for NO_2 and NH_4

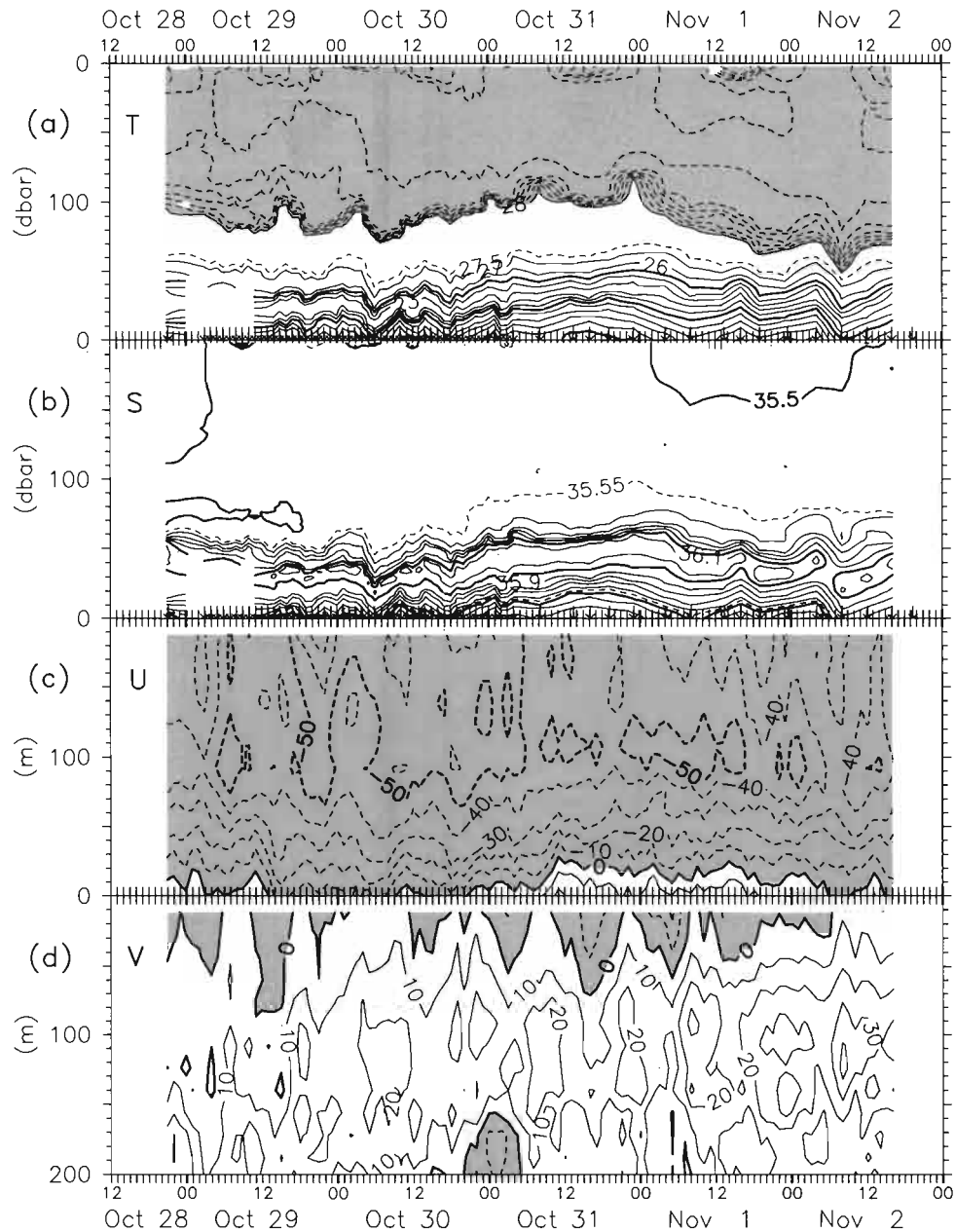


Figure 4. Temporal evolution of (a) temperature, (b) salinity, and (c) zonal and (d) meridional currents during the 5-day station at 3°S, 180°. Isolines as in Figure 2, with 0.1°C contours above 28°C and the 35.55 psu isohaline added. CTD casts shown by arrows. Note the denser sampling during the first 2 days.

which displayed monotonous temporal distributions with high maxima centered around 137 and 113 m, respectively (Figures 5b and 5c and Table 1). As noted earlier (section 3.1), the 3°S sampling station was in a zone of high remineralization. The 2 first days of intensive sampling (29–30 October) did not reveal any diurnal signal in the N nutrient fields, but some high-frequency variability was evident at the depth of NH_4 maximum for the whole station. A time series analysis was performed to check whether the semidiurnal hydrological oscillations could be involved here, but it did not provide statistically significant results, down to the deepest sampling depth (140 m).

[19] In summary, the time series sampling at 3°S took place during a period of relative stability with low variability

in the physical and nutrient properties. As a consequence, no important variation in plankton biomass and composition can be expected here.

3.3. Time Series Station at 0°, 180°

[20] In contrast to the results at 3°S, sections from the equatorial time series station (4 November, 1200, to 9 November, 0400) presented a more coherent pattern of variability in physical properties as well as in nutrients (Figures 6 and 7). Beginning around midday on 5 November, about 24 hours after the station started, the upper 80 m layer slightly warmed by about 0.2°C, with the salinity decreasing by 0.2 and the current shifting from 20 cm s⁻¹ westward to more than 80 cm s⁻¹ southwest-

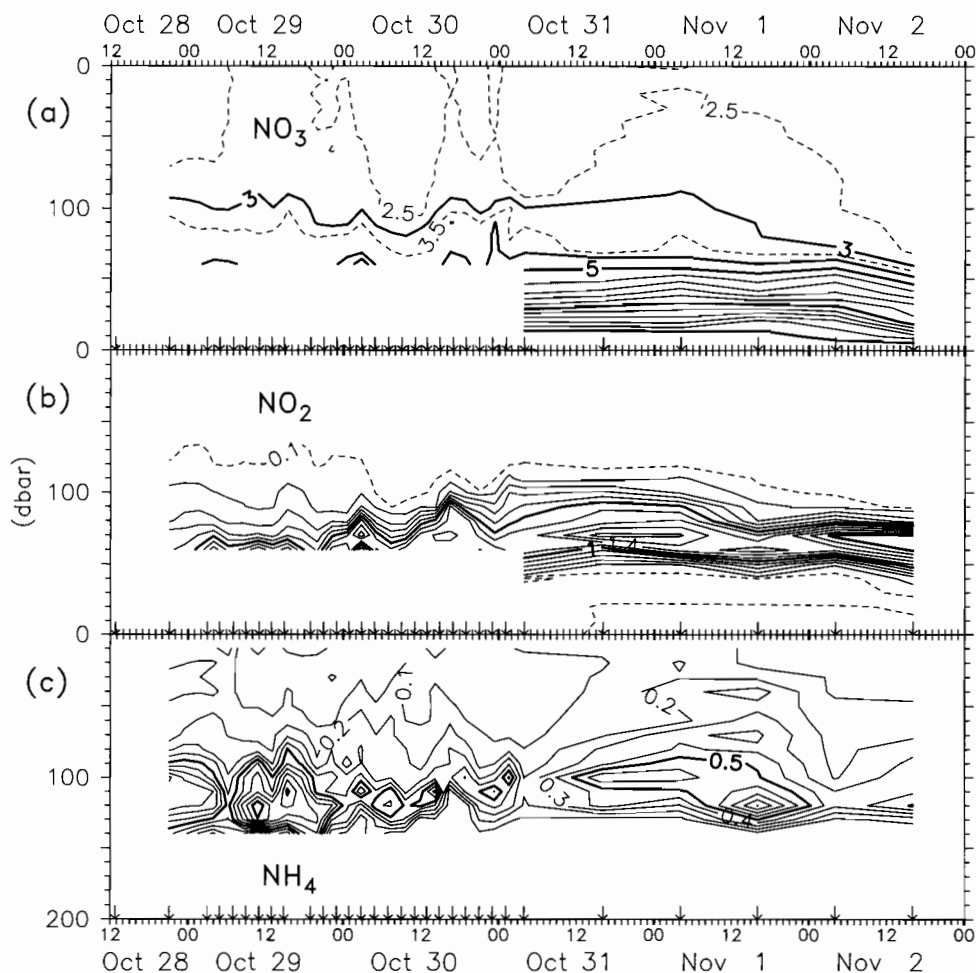


Figure 5. Temporal evolution of (a) nitrate, (b) nitrite, and (c) ammonia during the 5-day station at 3°S 180°. Isoline units are μM .

ward. At the same time, the EUC slightly increased by about 10 cm s^{-1} . These changes modified the structure of the upper oceanic layer by increasing thermohaline stratification. Superimposed on that stratification, a clear diurnal temperature cycle of $0.3 \text{ }^\circ\text{C}$ appeared near the surface and thickened to 40 m, reaching slightly deeper than at 3°S. During the first 2 days of high-frequency sampling, a strong semidiurnal cycle appeared in temperature and salinity fields below 100 m, with vertical displacements of isotherms and isohalines of 10–20 m amplitude. This cycle was also present in meridional velocity, with an amplitude of $10\text{--}20 \text{ cm s}^{-1}$ during the whole time series. It did not show on the second half of the hydrology sections probably only because of the lower sampling frequency.

[21] The appearance of higher temperatures and lower salinities on day 2 was associated with an abrupt decrease of nitrate in surface (from $3.7 \mu\text{M}$ to $1.7 \mu\text{M}$) and subsurface waters down to 90 m, and a decrease of nitrite. These N nutrients distributions were then stable for the remaining time of station sampling. In contrast, ammonium was nearly undetectable at the beginning of the time series (days 1–2) and increased after day 3, developing a smooth maximum of $0.2 \mu\text{M}$ at the top of the nitracline. On average, NH_4 and NO_2 concentrations at the equator were significantly lower

than at 3°S (Table 1), indicating a zone of low remineralization. Si(OH)_4 and PO_4 were sampled only during the second half of the time series and were found at that time as stable as N nutrients (not shown here) [see *Le Borgne et al.*, 1999].

[22] In contrast to 3°S, high-frequency variability measured by intensive profiling during the first two days (every 1–2 hours) at the equatorial time series station showed a

Table 1. Summary of Averaged (± 1 Std. Dev.) Hydrographic and Nutrient Parameters at the Two EBENE Time Series Stations^a

	Time Series at 3°S, 180°	Time Series at 0°, 180°
SST ($^\circ\text{C}$)	28.74 (± 0.14) $^\circ\text{C}$	28.09 (± 0.17) $^\circ\text{C}$
Surface NO_3 concentration	2.40 (± 0.17) μM	3.33 \rightarrow 1.77 μM
Mixed layer depth	109 (± 12) m	97 (± 16) m
1% Light depth	82 (± 6) m	78 (± 11) m
0.1% Light depth	134 (± 11) m	120 (± 9) m
NH_4 max: depth	113 (± 10) m	86 (± 11) m
NH_4 max: concentration	0.65 (± 0.20) μM	0.10 (± 0.06) μM
NO_2 max: depth	137 (± 6) m	98 (± 7) m
NO_2 max: concentration	1.47 (± 0.31) μM	0.51 (± 0.03) μM

^aThe mixed layer thickness is defined as the first depth where the density gradient exceeds 0.01 kg m^{-4} [Lukas and Lindstrom, 1991] after removing the surface layer affected by the diurnal cycle.

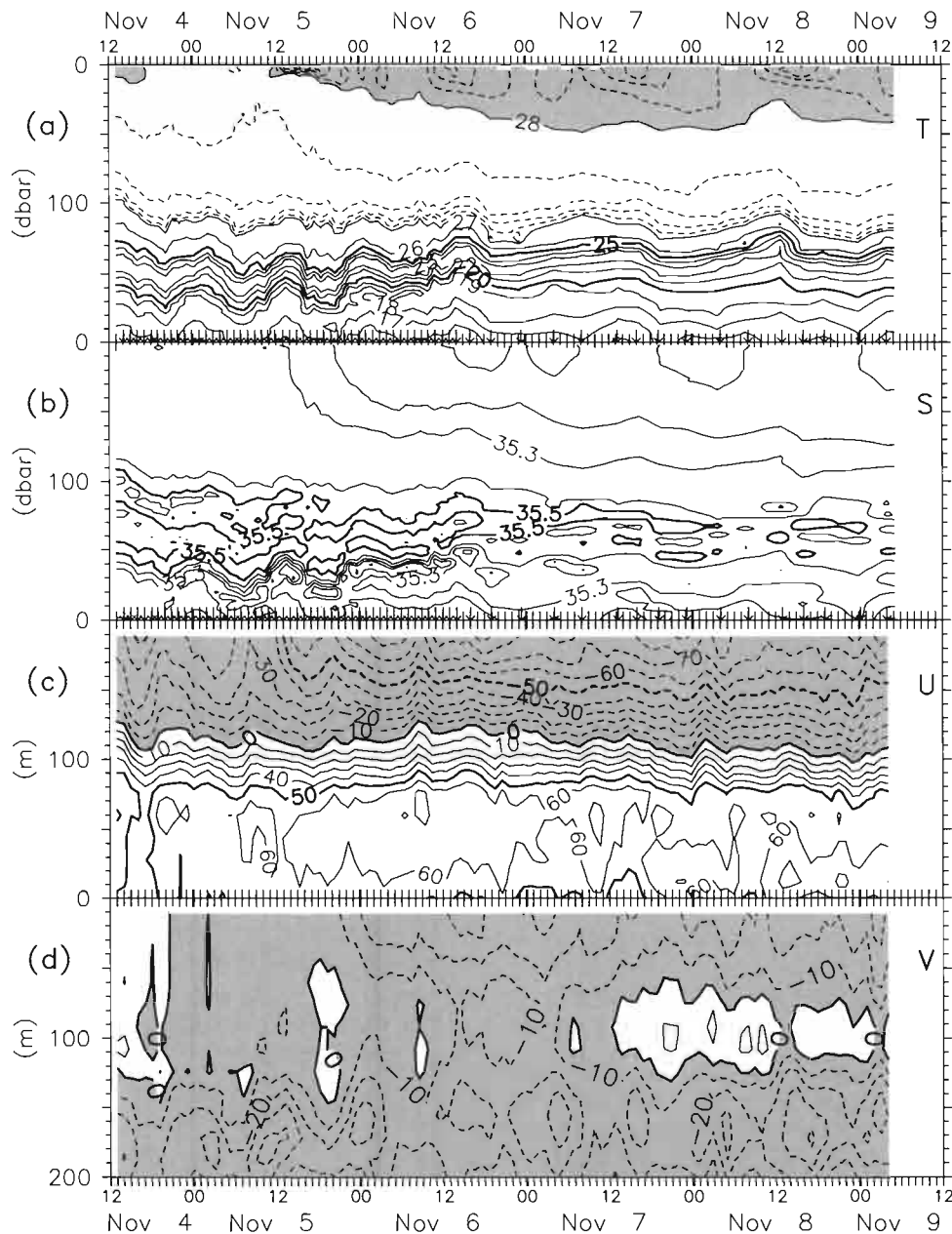


Figure 6. Temporal evolution of (a) temperature, (b) salinity, and (c) zonal and (d) meridional currents during the 5-day station at the equator, 180° . Contour intervals as in Figure 4.

significant semidiurnal cycle in NO_3 and NO_2 distributions below 100 m. These variations were consistent with physical observations, the NO_3 isolines depths varying up to 20 m. Conversely, neither diurnal nor semidiurnal cycles of N nutrients could be detected in the upper 100 m. High-frequency variability of NH_4 could not be resolved, because concentrations during the first 2 days remained too close to the limit of detection.

4. Discussion

[23] Given that the EBENE cruise took place at the end of the 1995–1996 cold phase of ENSO (La Niña), data from the TAO moorings array (not shown) allow us to outline some consequences of that large-scale climatic state at the

180° meridian. In the equatorial waveguide (2°S – 2°N), trade winds were above average ($+1$ – 2 m s^{-1} on monthly averages) from the first quarter of 1995 to November 1996. In the same period, SST cooled slightly (about -0.5°C) because of increased latent heat exchange with the atmosphere, and the thermocline deepened by about 10 m from the piling up of surface waters in the western Pacific. Because of the steady strong trade winds, equatorial upwelling was active and formed a wedge-shaped tongue penetrating warmer waters of the western Pacific Warm Pool, with the SST maxima centered at about 5° latitude on each side of the cold tongue (also shown in NCEP analyses; see Figure 1). Poleward of 5°S and 5°N , SST remained close to normal ($>28.5^\circ\text{C}$), with some seasonal variations in the northern hemisphere. At depth, the thermocline was not

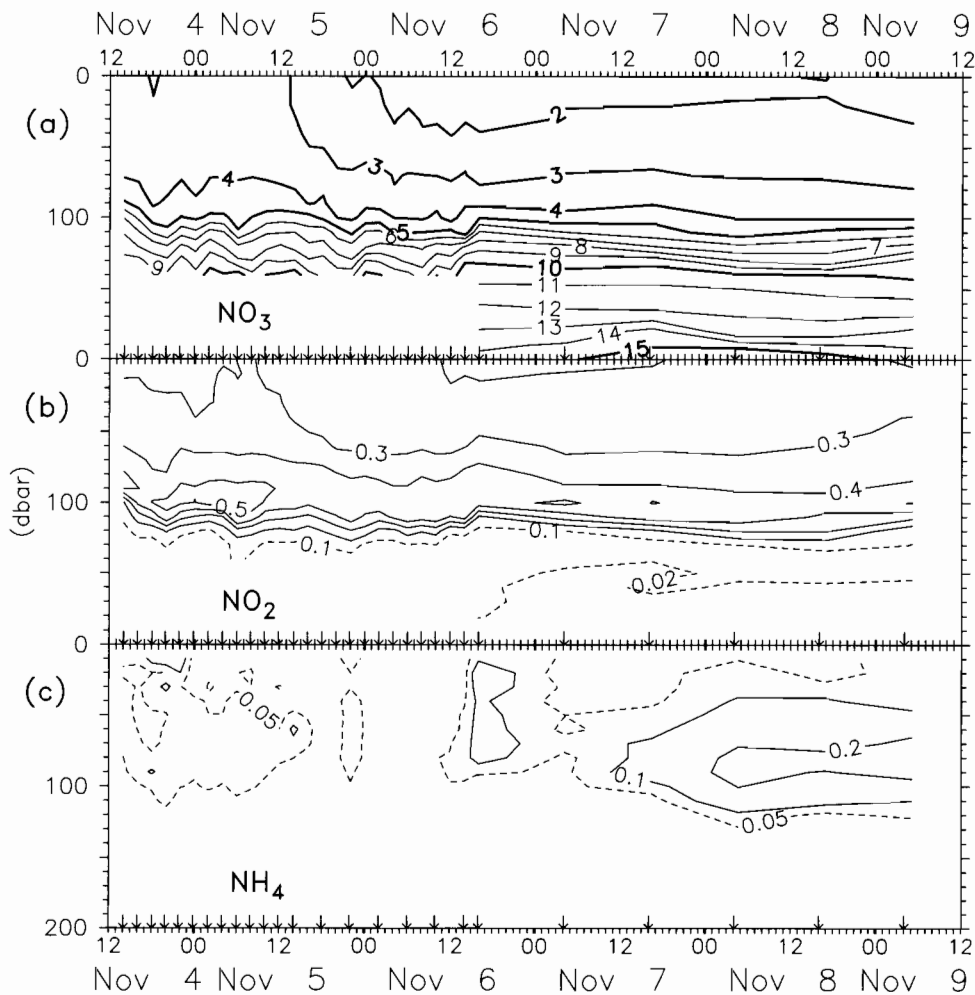


Figure 7. Temporal evolution of (a) nitrate, (b) nitrite, and (c) ammonia during the 5-day station at the equator, 180°. Units are μM .

much affected by La Niña in the south, but its seasonal cycle increased at 5°N with a stronger deepening in the boreal winter, leading to an increase in NECC flow [Kessler and Taft, 1987].

[24] Our observations from the cross-equatorial section are coherent with large-scale patterns of an active equatorial upwelling tongue, as defined above. The strong meridional asymmetry in the surface layer around the equator is addressed below in the discussion on the equatorial fixed station. Below the surface mixed layer, the asymmetry of hydrology or NO_3 is associated with the geostrophic signature of the zonal equatorial currents system and the corresponding isopycnal slopes. The meridional distribution of remineralization products (NO_2 and NH_4 ; Figures 3b and 3c) is directly linked to the dynamics of equatorial upwelling [Oudot, 1978]. On both sides of the equator the vertical density gradients (not shown) are similar, and remineralization products tend to accumulate above the maximum gradient, in the stablest layers of the thermocline. Because of the more energetic structures of oceanic circulation in the north (strong NECC and strong meridional shear between SEC and NECC), NO_2 and NH_4 are advected away and diluted faster than in the south, where they can reach higher concentrations. Differences in concentration

patterns of NO_3 and PO_4 (Figures 3a and 3d) imply variable NO_3/PO_4 molar ratio along the transect. This situation was previously observed at 150°W [Raimbault et al., 1999], and it suggests a relative deficit of NO_3 concentration in the southern and northern parts of the transect. To quantify how our results fit in the global context, a comparison with climatologies of the World Ocean Atlas of 1998 (WOA98, available from NODC/NOAA, USA) is presented in Figure 8 for temperature, salinity and nitrate in surface waters and at 100 m. South of 1°S, the temperature anomaly was close to 0 or negative at the surface but slightly positive at 100-m depth, indicating a relatively deep mixed layer. In the same area, the salinity anomaly was positive at the surface. Cooler SST and higher SSS are both characteristic of the cold phase of ENSO (La Niña), associated in the western Pacific with strong trade winds and less precipitation [Delcroix et al., 1996]. Between 1°S and the equator, T, S, and NO_3 confirm enhanced upwelling in the upper 100 m. Between the equator and 4°N, surface temperature was close to normal, but the anomaly was positive at depth. Salinity and especially NO_3 were below average in the whole surface layer. It is worth noting that the observed anomalies changed significantly during the 5-day station at 0°. North of 4°–5°N, the anomalous strong temperature

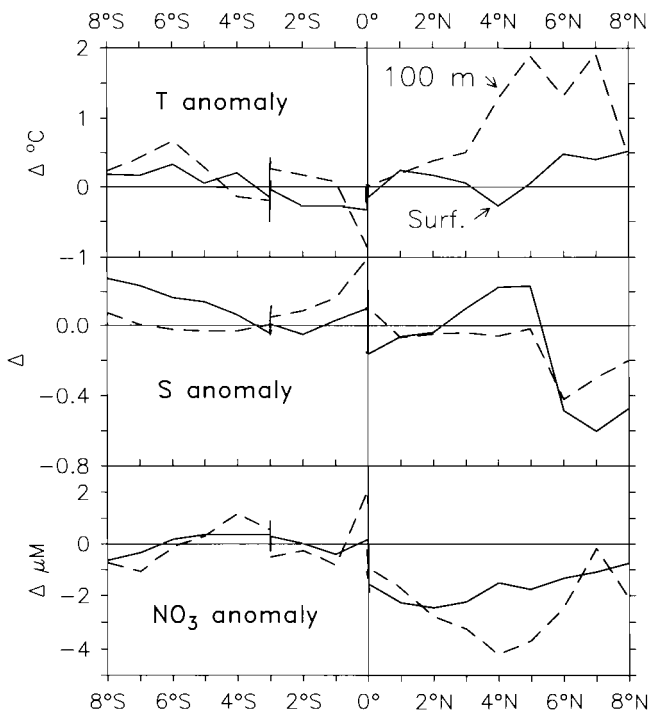


Figure 8. Anomalies of temperature, salinity, and nitrate concentration along the section at 180° in surface waters (solid line) and at 100 m depth (dashed line). Anomalies computed relative to NOAA WOA98 annual climatology. High-frequency variability during the 5-day stations at 3°S and 0° is noticeable.

gradient at 100 m and the anomalous freshening of the 0–100 m layer were signatures of a stronger than average NECC. The 1.5°C temperature anomaly at $4^\circ\text{--}5^\circ\text{N}$ confirmed an anomalous deepening of the surface layer corresponding to strong horizontal convergence, already hinted in Figure 2a. Thus it appears that most of the observed anomalies reflected La Niña conditions, except for north of the equator, which was more affected by higher-frequency variability.

[25] To better understand variability at the equator, as described in section 3.3, Figure 9 presents averages of physical parameters and NO_3 above 80 m, inside the mixed layer during the station (see Table 1). During the first 2 days, surface winds decreased while surface currents increased to the southwest, and there was no apparent relation between local forcing and current variation. The observed trends in temperature and salinity cannot be explained either by local heat or water exchange with the atmosphere. The wind did not decrease enough to significantly impact local heat fluxes, and rainfall stayed negligible during the station. Given the insignificant effects of local forcing, horizontal advection of an 80-m layer of relatively warm, fresh and nitrate-impoverished water from the northeast might explain the observed changes. The abrupt decrease of NO_3 after the 1st day, as well as the very low surface NO_3 gradient observed north of the equator over 5 degrees support this idea. For example, it is clear that biological processes alone (i.e., nitrate uptake) can not account for the observed decrease of NO_3 in the upper 80 m ($120.5 \text{ mmol N m}^{-2} \text{ d}^{-1}$). Indeed, during the cruise an NO_3 uptake rate of only

$3.6 \text{ mmol N m}^{-2} \text{ d}^{-1}$ was measured at the equator, [Le Bouteiller *et al.*, 2003] which already is at the high end of uptake ranges previously measured in the area, $0.7\text{--}3.8 \text{ mmol N m}^{-2} \text{ d}^{-1}$ [McCarthy *et al.*, 1996; Raimbault *et al.*, 1999; Aufdenkampe *et al.*, 2002] The NH_4 increase observed during the second half of the time series station (Figure 7c) is also consistent with the advective hypothesis, assuming that a southward flow brings water from the north of the area, which is usually NH_4 -enriched by remineralization. The 1-day time lag between the decrease in NO_3 and the increase in NH_4 is coherent with the fact that heterotrophic biomass associated with the remineralization process exceeded the autotroph biomass (“inverted structure”) north of 1°N [Brown *et al.*, 2003].

[26] The rapid decrease of salinity and nitrate on 5 November, representing about 80% of its total amplitude in just 12 hours, provides another clue about the presumptive advective mechanism. Assuming meridional advection, for instance, the observed parameter gradients and measured meridional velocity (i.e., a $1 \mu\text{M deg}^{-1} \text{NO}_3$ gradient times $0.2^\circ\text{C deg}^{-1}$ meridional velocity) suggest that several days would be needed to affect the changes that actually occurred in a matter of hours. Therefore large-scale meridional advection alone cannot explain the rapid changes. Hence we suppose that a frontal structure delineates the fresher water mass and that we observed its transit across the equator on 5 November. Our hypothesis is that these features are part of the southward branch of a Tropical Instability Wave (TIW) where frontal structures are common [Archer *et al.*, 1996].

[27] Fully developed TIWs form anticyclonic current eddies north of the equator, with a northward branch exporting upwelled water away from the equator, and a southward branch bringing warmer and fresher water back to the equator [Flament *et al.*, 1996]. To our knowledge, TIWs have not been described yet so far in the western Pacific, and some additional evidence is needed. Temperature records from the TAO buoys at 180° cannot show variability at TIW periodicity (15–35 days), because of the weak temperature gradients in the area. The closest surface current record comes from the $0^\circ, 170^\circ\text{W}$ buoy, and Figure 10a presents this data for the whole time span of available data, 1988–1997. TIW activity is noticeable by oscillations at 15–35 days in the meridional velocity field, and appears to have been most significant at 170°W only during cold episodes, in 1988–1989 and 1995–1996. Other episodes of lesser amplitude occurred in 1992 and 1994.

[28] TIWs are generated by shear instabilities at boundaries between currents of the equatorial circulation system. During cold episodes, the SEC and NECC are reinforced in the central Pacific, so that TIWs can be generated farther west than at other times, and thus also propagate farther west. Figure 10b shows details of the same data as well as $0^\circ, 180^\circ$ SST for the 1995–1996 period. TIW meridional velocity oscillations are clear at least from September to December 1996, but they do not show in SST, as stated earlier, either at 170°W or 180° . From data at 140°W , Qiao and Weisberg [1995] estimated the TIW period to be centered at 20.8 days, with a wavelength of 900 to 1300 km. Assuming that their results are still valid at 170°W to 180° (which is not completely confirmed) [see Masina and Philander, 1999], one can deduce from the date

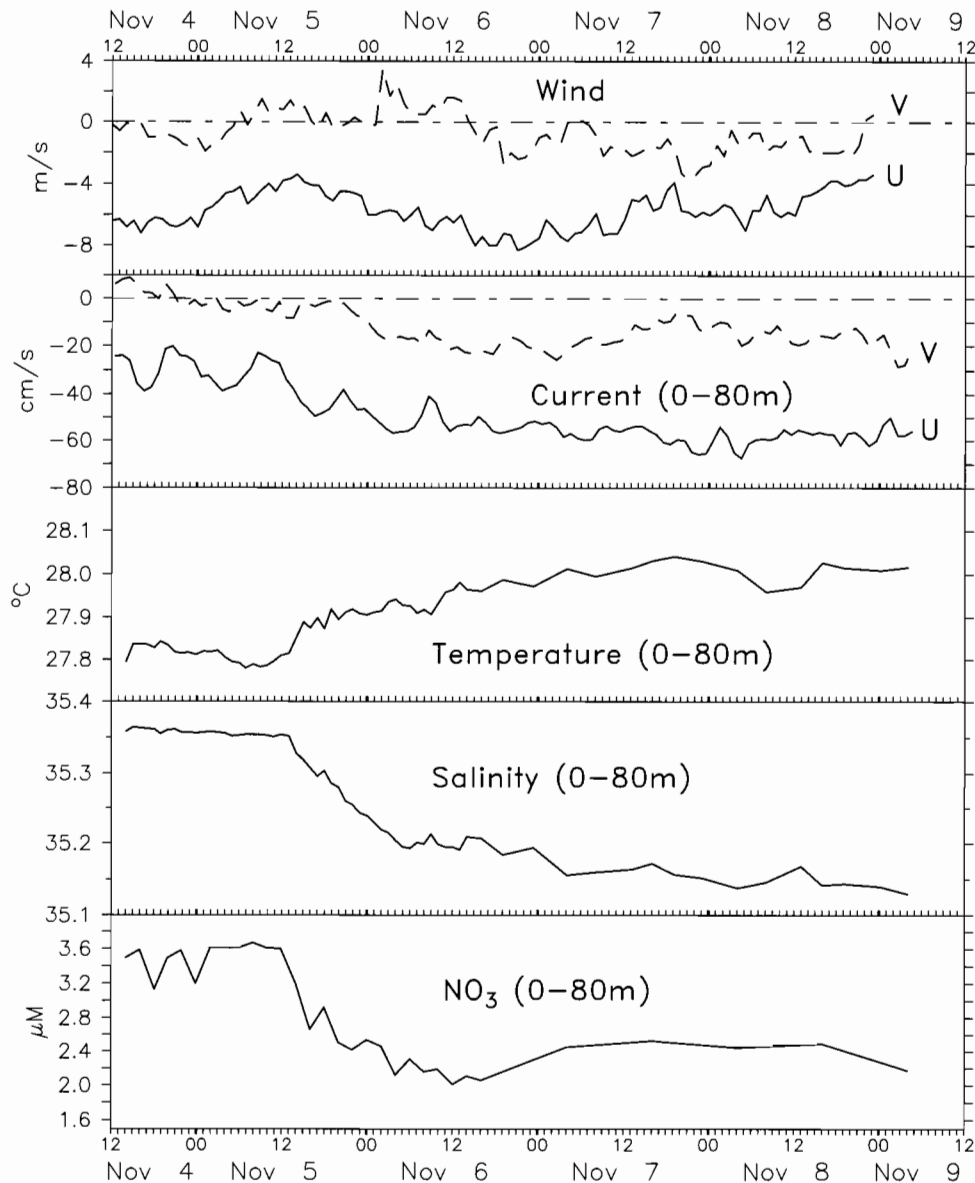


Figure 9. Variability of surface winds, currents, temperature, salinity, and nitrate during the 5-day time series station at 0° , 180° . Surface wind components (U, eastward; V, northward) are from the TAO mooring. Current components (U, eastward; V, northward), temperature, salinity, and NO_3 are 0–80 m averages from cruise data.

of reversal of meridional flow (from north to south) at 170°W on 6 November, the date of that change at 180° . Depending on the wavelength used, that date would be between 3 and 11 November, which agrees with our observations of 5 November.

[29] In addition to the TIW signal in Figure 10b, the U velocity component shows some variability at a 40–60 day period from July to December 1996, with decreases or even reversals of the westward current at that periodicity. Some SST increases of about 1°C amplitude are also noticeable at 170°W , but not at 180° . Detailed study of that variability is out of the scope of the present paper, but observations from the TAO array (not shown, available at <http://www.pmel.noaa.gov/tao/jsdisplay/>) indicate that periodic zonal current decreases coincide with a deepening of the 20°C isotherm, which is the signature of intraseasonal Kelvin

waves [Kessler *et al.*, 1995]. Probably because of nonnegligible zonal temperature gradients at 170°W , propagation of each of the waves is associated with an SST warming, but at 180° these waves do not affect SST (Figure 10b). They are of weak amplitude compared to previous observations in the area [Eldin *et al.*, 1997]. Moreover, the EBENE equatorial station sampled between two of these waves, as shown on Figure 10b, so that associated velocity field and thermocline depth were not very different from long-term averages. We thus suppose that they did not have much influence on our nutrient observations.

[30] The TIW consequences are clearly seen in physical and chemical parameters, but their effect on the trophic chain is not so straightforward. Biological aspects are detailed in other papers of this special issue, but some examples are worth citing here. First, in spite of the NO_3

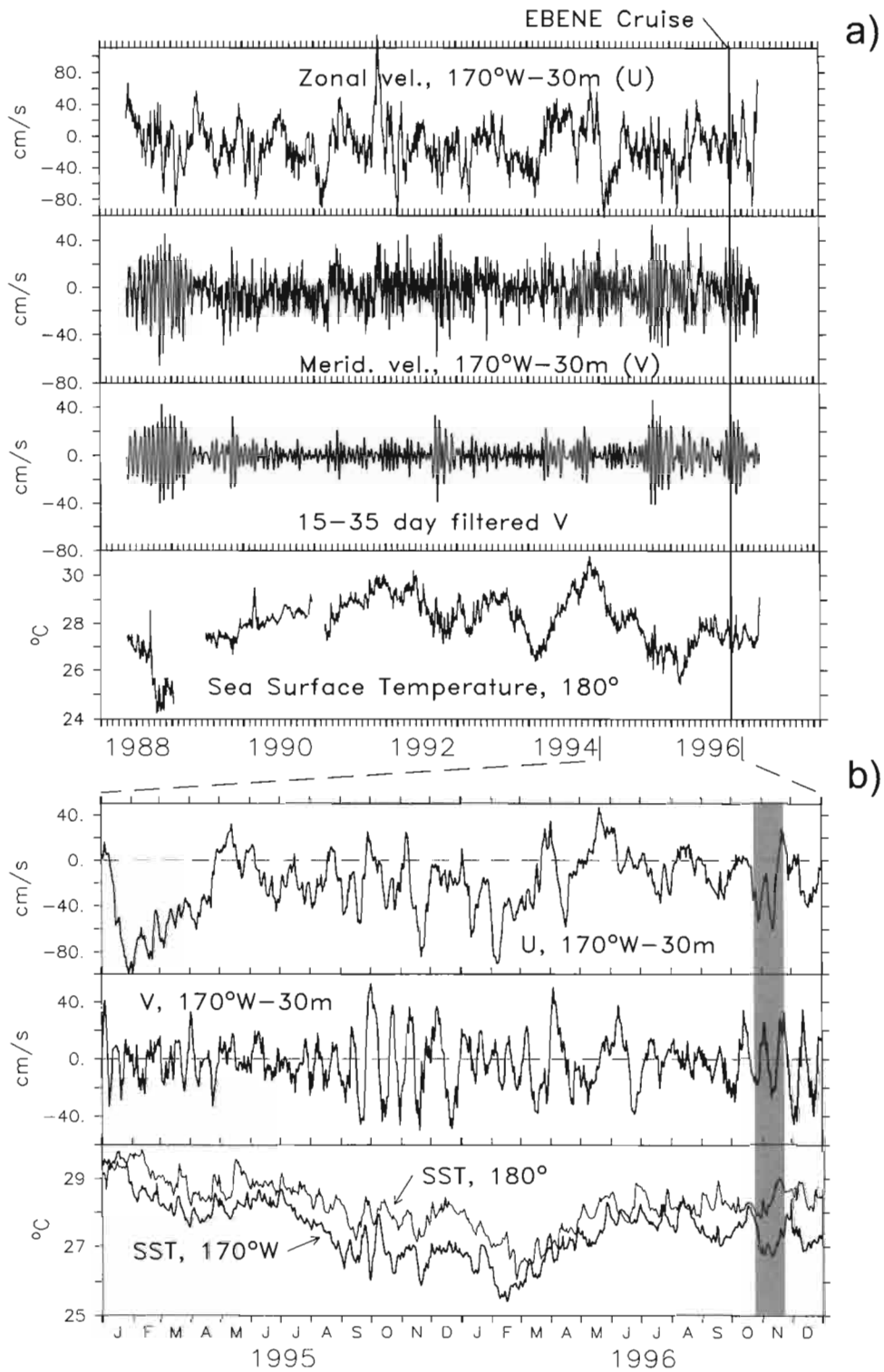


Figure 10. (a) Daily averaged zonal, meridional, and filtered currents and sea surface temperature from the 0°, 180° TAO mooring from 1988 to 1997. All current components at 30 m; meridional component after filtering by a 15–35 days Butterworth filter. (b) Same data for 1995–1996 only, without filtered V and with SST from the 0°, 170°W mooring added.

decrease at the TIW passage, phytoplankton biomass levels (in terms of integrated chlorophyll) did not significantly change during the 5-day equatorial station excepted in the upper 20 m [Neveux *et al.*, 2003]. Second, while primary production [Le Bouteiller *et al.*, 2003] and components of

phytoplankton communities [Brown *et al.*, 2003] in the equatorial band were equivalent inside and outside of the southward current branch of the TIW, Brown *et al.* [2003] describe a peculiar “inverted” trophic structure in that branch, suggesting a change in the food web structure.

Finally, according to *Le Borgne et al.* [2003], the TIW passage could also explain the low mesozooplankton biomass observed north of the equator and therefore the latitudinal asymmetry in zooplankton distribution.

[31] Our results contrast with most previous observations made at the equator on variability associated with TIWs. During EqPac cruise TT012 (October 1992), for instance, nitrate, chlorophyll, and primary production increased as temperature decreased as a TIW went past [Murray *et al.*, 1994; Barber *et al.*, 1996; Foley *et al.*, 1997], in association with a maximum northward current. Increases in microzooplankton [Verity *et al.*, 1996] and mesozooplankton biomass were also reported, although they lagged behind the increase in nutrients and chlorophyll by several days [Roman *et al.*, 1995]. The effects were explained by the increases in upwelling and vertical mixing found in the northward branch of TIWs. Our data show that opposite effects can be evidenced in the other half of the TIW eddy, mainly on physical and chemical parameters.

[32] At higher frequency, the two time series stations revealed a diurnal cycle in surface temperatures. This cycle was of larger amplitude on the equator than at 3°S and was fully generated by the diurnal cycle of solar radiance. Because the surface layer was homogeneous in nutrients, daily vertical stratification and nighttime mixing did not affect nutrient distributions during the time series stations. The well-known diurnal cycle in primary producers will be dealt with by other papers [Neveux *et al.*, 2003]. Within and below the euphotic zone down to 140 m, it was not possible to detect any diel cycle in the processes of remineralization linked to bacterial or zooplankton activities.

[33] The semidiurnal cycle of internal waves was most evident in meridional velocity records at both time series stations, at depth but also in surface at 3°S, during times of hourly sampling. This cycle was present in the thermocline and halocline, but could not be ascertained in nutrients data, mostly because intensive sampling did not reach deep enough in the thermocline. Internal waves change the depth of the thermocline and can increase mixing, and for that reason may act on the supply of nutrients to the euphotic layer [Mackey *et al.*, 1997]. It does not seem to be the case here, probably because the wave amplitude was too weak at the base of the euphotic layer.

5. Conclusions

[34] Data from the EBENE cruise have allowed a description of physical and nutrients properties in the western extremity of the Pacific Ocean equatorial upwelling during cold conditions of the ENSO cycle. Intensive sampling at two 5-day time series stations has provided some insight on high-frequency variability, and particularly on the effects of TIWs at the equator. Under these conditions and at the timescale of a few days, nutrient distributions were mainly controlled by physical processes rather than by biological activity. In contrast to previous observations, TIWs can contribute to a relative decrease of nutrients at the equator, depending on the phase of the wave at the time and longitude of observation. Consequences on the trophic web at the equator are not straightforward and rather affect the microbial community structure, with changes in higher trophic levels than the phytoplankton biomass or primary

production, as shown in other papers of this special issue. To our knowledge, there is no previous published report of observations in a well identified southern branch of a TIW; more complete studies on larger timescales and spatial scales are needed to understand and quantify a complete budget of nutrient variability and transport processes during both the enrichment and impoverishment phases of the wave eddy.

[35] Even if theoretically feasible, higher-frequency nutrient variability (at infradiurnal periods) could not be adequately described with 2-hour and 10–20 m sampling. For that purpose, moored instrumentation and high temporal resolution measurements of physical, chemical and biological variables would be needed.

[36] **Acknowledgments.** The assistance and efforts of officers and crew of R/V *L'Atalante* from IFREMER were greatly appreciated. We would also like to thank our chief scientist, Robert Le Borgne. Measurements and analyses at sea were performed with the invaluable help of Philippe Gérard and Laurent Veyseyre. Financial support for this work was provided by IRD and INSU-CNRS.

References

- Archer, D. E., T. Takahashi, S. Sutherland, J. Goddard, D. Chipman, K. Rodgers, and H. Ogura, Daily, seasonal and interannual variability of phytoplankton pigment distributions in the central equatorial Pacific Ocean, *Deep Sea Res., Part II*, 43, 779–808, 1996.
- Aufdenkampe, A. K., J. J. Mc Carthy, C. Navarette, M. Rodier, J. Dunne, and J. W. Murray, Biogeochemical controls on new production in the tropical Pacific, *Deep Sea Res., Part II*, 49, 2619–2648, 2002.
- Bahr, F., E. Firing, and S. Jiang, Acoustic Doppler current profiling in the western Pacific during the US-PRC TOGA cruises 2, 3 and 4, *JIMAR Data Rep.* 5, 199 pp., Univ. of Hawaii, Honolulu, 1989.
- Barber, R. T., and J. E. Kogelschatz, Nutrient and productivity during the 1982/83 El Niño, in *Global Ecological Consequences of the 1982–83 El Niño-Southern Oscillation*, edited by P. W. Glynn, pp. 21–53, Elsevier, New York, 1989.
- Barber, R. T., M. P. Sanderson, S. T. Lindley, F. Chai, J. Newton, C. C. Trees, D. G. Foley, and F. P. Chavez, Primary productivity and its regulation in the equatorial Pacific during and following the 1991–1992 El Niño, *Deep Sea Res., Part II*, 43, 933–969, 1996.
- Bonnet, S., Manuel d'analyses chimiques dans l'eau de mer, *Arch. Sci. Mer Oceanogr. Phys. Cent. ORSTOM Noumea*, 2, 40 pp., 1995.
- Brown, S. L., M. R. Landry, J. Neveux, and C. Dupouy, Microbial community abundance and biomass along a 180° transect in the equatorial Pacific during an El Niño-Southern Oscillation cold phase, *J. Geophys. Res.*, 108(C12), 8139, doi:10.1029/2001JC000817, in press, 2003.
- Chavez, F. P., P. G. Strutton, G. E. Friederich, R. A. Feely, G. C. Feldman, D. G. Foley, and M. J. McPhaden, Biological and chemical response of the equatorial Pacific Ocean to the 1997–98 El Niño, *Science*, 286, 2126–2131, 1999.
- Delcroix, T., and C. Hénin, Observations of the equatorial intermediate current in the western Pacific Ocean (165°E), *J. Phys. Oceanogr.*, 18, 363–366, 1988.
- Delcroix, T., C. Hénin, V. Porte, and P. Arkin, Precipitation and sea-surface salinity in the tropical Pacific Ocean, *Deep Sea Res., Part I*, 43, 1123–1141, 1996.
- Eldin, G., M. Rodier, and M.-H. Radenac, Physical and nutrient variability in the upper equatorial Pacific, *Deep Sea Res., Part II*, 44, 1783–1800, 1997.
- Eriksen, C., Equatorial waves vertical modes observed in a western Pacific island array, *J. Phys. Oceanogr.*, 12, 1206–1220, 1982.
- Flament, P. J., S. C. Kennan, R. A. Knox, P. P. Niiler, and R. L. Bernstein, The three-dimensional structure of an upper ocean vortex in the tropical Pacific Ocean, *Nature*, 383, 610–613, 1996.
- Foley, D. G., T. D. Dickey, M. J. McPhaden, R. R. Bidigare, M. R. Lewis, R. T. Barber, S. T. Lindley, C. Garside, D. V. Manov, and J. D. McNeil, Longwaves and primary productivity variations in the equatorial Pacific at 0°, 140°W, *Deep Sea Res., Part II*, 44, 1801–1826, 1997.
- Gourdeau, L., Internal tides observed at 2°S–156°E during COARE, *J. Geophys. Res.*, 103, 12,629–12,638, 1998.
- Kessler, W. S., and B. A. Taft, Dynamic heights and zonal geostrophic transports in the central tropical Pacific during 1979–84, *J. Phys. Oceanogr.*, 17, 97–122, 1987.

- Kessler, W. S., M. J. McPhaden, and K. M. Weickmann, Forcing of intraseasonal Kelvin waves in the equatorial Pacific, *J. Geophys. Res.*, **100**, 10,613–10,631, 1995.
- Le Borgne, R., M.-J. Langlade, P. Polidori, and M. Rodier, Campagne océanographique EBENE à bord du N. O. l'ATALANTE 21 Octobre–20 Novembre 1996 Recueil de données. tome 1: Météorologie, courantologie, données de surface, hydrologie, sels nutritifs et phytoplancton, *Arch. Sci. Mer Oceanogr. Phys. Cent. ORSTOM Noumea*, **1**, 1–30, 1998.
- Le Borgne, R., M. Rodier, A. Le Bouteiller, and J. W. Murray, Zonal variability of plankton and particle export flux in the equatorial Pacific upwelling between 165°E and 150°W, *Oceanol. Acta*, **22**, 57–66, 1999.
- Le Borgne, R., and M. R. Landry, EBENE: A JGOFS investigation of plankton variability and trophic interactions in the equatorial Pacific (180°), *J. Geophys. Res.*, **108**(C12), 8136, doi:10.1029/2001JC001252, in press, 2003.
- Le Borgne, R., G. Champalbert, and R. Gaudy, Mesozooplankton biomass and composition in the equatorial Pacific along 180°, *J. Geophys. Res.*, **108**(C12), 8143, doi:10.1029/2000JC000745, 2003.
- Le Bouteiller, A., A. Leynaert, M. Landry, R. Le Borgne, J. Neveux, M. Rodier, J. Blanchot, and S. Brown, Primary production, new production, and growth rate in the equatorial Pacific: Changes from mesotrophic to oligotrophic regime, *J. Geophys. Res.*, **108**(C12), 8141, doi:10.1029/2000JC000914, in press, 2003.
- Leynaert, A., P. Tréguer, C. Lancelot, and M. Rodier, Silicon limitation in the equatorial Pacific: Evidence from Si uptake kinetics studies, *Deep Sea Res.*, **Part 1**, **48**, 639–660, 2001.
- Lukas, R., and E. Lindstrom, The mixed layer of the western equatorial Pacific Ocean, *J. Geophys. Res.*, **96**, 3343–3357, 1991.
- Mackey, D. J., J. Parslow, F. B. Griffiths, H. W. Higgins, and B. Tilbrook, Phytoplankton productivity and the carbon cycle in the western equatorial Pacific under El Niño and non-El Niño conditions, *Deep Sea Res.*, **Part 2**, **44**, 1951–1978, 1997.
- Magnier, Y., H. Rotschi, P. Rual, and C. Colin, Equatorial circulation in the western Pacific, *Prog. Oceanogr.*, **6**, 29–46, 1973.
- Masina, S., and S. G. H. Philander, An analysis of tropical instability waves in a numerical model of the Pacific Ocean: 1. Spatial variability of the waves, *J. Geophys. Res.*, **104**, 29,613–29,635, 1999.
- McCarthy, J. J., C. Garside, and J. L. Nevins, New production along 140°W in the equatorial Pacific during and following the 1992 El Niño, *Deep Sea Res.*, **Part 2**, **43**, 1065–1093, 1996.
- McPhaden, M. J., and S. Hayes, Variability in the eastern equatorial Pacific Ocean during 1986–1988, *J. Geophys. Res.*, **95**, 13,195–13,208, 1990.
- McPhaden, M. J., and B. A. Taft, On the dynamics of seasonal and intra-seasonal variability in the eastern equatorial Pacific, *J. Phys. Oceanogr.*, **18**, 1713–1732, 1988.
- Minas, H. J., M. Minas, and T. T. Packard, Productivity in upwelling areas deduced from hydrographic and chemical fields, *Limnol. Oceanogr.*, **31**, 1182–1206, 1986.
- Murray, J. W., R. T. Barber, M. R. Roman, M. P. Bacon, and R. A. Feely, Physical and biological controls on carbon cycling in the equatorial Pacific, *Science*, **266**, 58–65, 1994.
- Murray, J. W., E. Johnson, and C. Garside, A U. S. JGOFS Process Study in the equatorial Pacific (EqPac): Introduction, *Deep Sea Res.*, **Part 2**, **42**, 275–293, 1995.
- Neveux, J., C. Dupouy, J. Blanchot, A. Le Bouteiller, M. R. Landry, and S. L. Brown, Diel dynamics of chlorophylls in high-nutrient, low-chlorophyll waters of the equatorial Pacific (180°): Interactions of growth, grazing, physiological responses, and mixing, *J. Geophys. Res.*, **108**(C12), 8140, doi:10.1029/2000JC000747, in press, 2003.
- Oudot, C., Continuité zonale et circulation méridienne du maximum de nitrite dans le Pacifique équatorial sud-ouest. I. Description de l'évolution spatiale du maximum de nitrite dans le contexte hydrologique, *Cah. ORSTOM Ser. Oceanogr.*, **16**, 349–361, 1978.
- Peters, H., M. C. Gregg, and T. B. Stanford, The diurnal cycle of the upper equatorial ocean: Turbulence, fine-scale shear, and mean shear, *J. Geophys. Res.*, **99**, 7707–7723, 1994.
- Picaut, J., M. Ioualalen, C. Menkes, T. Delcroix, and M. J. McPhaden, Mechanisms of the zonal displacements of the Pacific warm pool: Implications for ENSO, *Science*, **274**, 1486–1489, 1996.
- Qiao, L., and R. H. Weisberg, Tropical instability wave kinematics: Observations from the Tropical Instability Wave Experiment (TIWE), *J. Geophys. Res.*, **100**, 8677–8693, 1995.
- Radenac, M.-H., and M. Rodier, Nitrate and chlorophyll distributions in relation to thermohaline and current structures in the western tropical Pacific during 1985–1989, *Deep Sea Res.*, **Part 2**, **43**, 725–752, 1996.
- Raimbault, P., G. Slawyck, B. Boudjellal, C. Coatanoan, P. Conan, B. Coste, N. Garcia, T. Moutin, and M. Pujo-Pay, Carbon and nitrogen uptake and export in the equatorial Pacific at 150°W: Evidence of an efficient regenerated production cycle, *J. Geophys. Res.*, **104**, 3341–3356, 1999.
- Reynolds, R. W., and T. M. Smith, Improved global sea surface temperature analyses, *J. Climate*, **7**, 929–948, 1994.
- Roman, M. R., H. G. Dam, A. L. Gauzens, J. Urban-Rich, D. G. Foley, and T. D. Dickey, Zooplankton variability on the equator at 140°W during the JGOFS EqPac study, *Deep Sea Res.*, **Part 2**, **42**, 673–693, 1995.
- Trenberth, K. E., and J. W. Hurrell, Decadal atmosphere-ocean variations in the Pacific, *Clim. Dyn.*, **9**, 303–319, 1994.
- Tsuchiya, M., Upper waters of the intertropical Pacific Ocean, *Johns Hopkins Oceanogr. Stud.*, **4**, 50 pp., 1968.
- Turk, D., M. R. Lewis, W. G. Harrison, T. Kawano, and I. Asanum, Geographical distribution of new production in the western/central equatorial Pacific during El Niño and normal conditions, *J. Geophys. Res.*, **106**, 4501–4515, 2001.
- Verity, P. G., D. K. Stoecker, M. E. Sieracki, and J. R. Nelson, Microzooplankton grazing of primary production at 140°W in the equatorial Pacific, *Deep Sea Res.*, **Part 2**, **43**, 1227–1255, 1996.
- Wyrtki, K., and B. Kilonsky, Mean water and current structure during the Hawaii-to-Tahiti Shuttle Experiment, *J. Phys. Oceanogr.*, **14**, 242–254, 1984.

G. Eldin, LEGOS (CNES, CNRS, IRD, UPS), 14 Avenue Edouard Belin, 31400 Toulouse, France. (gerard.eldin@cnes.fr)
M. Rodier, Centre IRD, BP A5, 98848 Nouméa, New Caledonia.

Eldin Gérard, Rodier Martine. (2003).

Ocean physics and nutrient fields along 180° during an El Nino-Southern Oscillation cold phase.

In : A JGOFS investigation of plankton variability and trophic interactions in the central equatorial Pacific (EBENE).

Journal of Geophysical Research, 108 (C12), 2-1 - 2-13. ISSN 0148-0227